

AFRL-ML-WP-TR-2001-4176

**POLYMER MATRIX COMPOSITE (PMC) DAMAGE
TOLERANCE AND REPAIR TECHNOLOGY**

RAN Y. KIM

**UNIVERSITY OF DAYTON RESEARCH INSTITUTE
300 COLLEGE PARK AVENUE
DAYTON, OH 45469-0168**



APRIL 2001

FINAL REPORT FOR PERIOD 15 SEPTEMBER 1999 – 1 MARCH 2001

Approved for public release; distribution unlimited.

**MATERIALS AND MANUFACTURING DIRECTORATE
AIR FORCE RESEARCH LABORATORY
AIR FORCE MATERIEL COMMAND
WRIGHT-PATTERSON AIR FORCE BASE, OH 45433-7750**

NOTICE

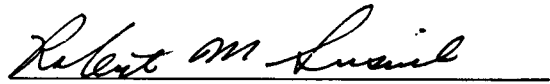
Using Government drawings, specifications, or other data included in this document for any purpose other than Government procurement does not in any way obligate the U.S. Government. The fact that the Government formulated or supplied the drawings, specifications, or other data does not license the holder or any other person or corporation; or convey any rights or permission to manufacture, use, or sell any patented invention that may relate to them.

This report is releasable to the National Technical Information Service (NTIS). At NTIS, it will be available to the general public, including foreign nations.

This technical report has been reviewed and is approved for publication.



L. SCOTT THEIBERT, Chief
Structural Materials Branch
Nonmetallic Materials Division



ROBERT M. SUSNIK, Deputy Chief
Nonmetallic Materials Division
Materials and Manufacturing Directorate

Do not return copies of this report unless contractual obligations or notice on a specific document requires its return.

REPORT DOCUMENTATION PAGE				<i>Form Approved</i> <i>OMB No. 0704-0188</i>	
The public reporting burden for this collection of information is estimated to average 1 hour per response, including the time for reviewing instructions, searching existing data sources, gathering and maintaining the data needed, and completing and reviewing the collection of information. Send comments regarding this burden estimate or any other aspect of this collection of information, including suggestions for reducing this burden, to Department of Defense, Washington Headquarters Services, Directorate for Information Operations and Reports (0704-0188), 1215 Jefferson Davis Highway, Suite 1204, Arlington, VA 22202-4302. Respondents should be aware that notwithstanding any other provision of law, no person shall be subject to any penalty for failing to comply with a collection of information if it does not display a currently valid OMB control number. PLEASE DO NOT RETURN YOUR FORM TO THE ABOVE ADDRESS.					
1. REPORT DATE (DD-MM-YY) April 2001		2. REPORT TYPE Final		3. DATES COVERED (From - To) 09/15/1999 – 03/01/2001	
4. TITLE AND SUBTITLE POLYMER MATRIX COMPOSITE (PMC) DAMAGE TOLERANCE AND REPAIR TECHNOLOGY				5a. CONTRACT NUMBER F33615-95-D-5029	
				5b. GRANT NUMBER (blank)	
				5c. PROGRAM ELEMENT NUMBER 62102F	
6. AUTHOR(S) RAN Y. KIM				5d. PROJECT NUMBER 4347	
				5e. TASK NUMBER 34	
				5f. WORK UNIT NUMBER 10	
7. PERFORMING ORGANIZATION NAME(S) AND ADDRESS(ES) UNIVERSITY OF DAYTON RESEARCH INSTITUTE 300 COLLEGE PARK DAYTON, OH 45469-0168				8. PERFORMING ORGANIZATION REPORT NUMBER UDR-TR-2001-00041	
9. SPONSORING/MONITORING AGENCY NAME(S) AND ADDRESS(ES) MATERIALS AND MANUFACTURING DIRECTORATE AIR FORCE RESEARCH LABORATORY AIR FORCE MATERIEL COMMAND WRIGHT-PATTERSON AIR FORCE BASE, OH 45433-7750				10. SPONSORING/MONITORING AGENCY ACRONYM(S) AFRL/MLBC	
				11. SPONSORING/MONITORING AGENCY REPORT NUMBER(S) AFRL-ML-WP-TR-2001-4176	
12. DISTRIBUTION/AVAILABILITY STATEMENT Approved for public release; distribution unlimited.					
13. SUPPLEMENTARY NOTES					
14. ABSTRACT (Maximum 200 Words) The application of composites in space structures such as reusable launch vehicles requires a detailed understanding of their mechanical behavior and damage resistance in the service environment. Experimental and analytical studies were conducted on IM7/977-3, a graphite-toughened epoxy, to characterize the influence of cryogenic service temperatures on the strength, modulus, and fracture of this material system, and on transverse crack initiation in cross-ply laminates at 23, -129, and -196 °C. Transverse tensile and shear strengths and moduli increased at the cryogenic test temperatures while strain to failure decreased, denoting increased brittleness. The stress for the onset of transverse cracking decreased substantially at cryogenic temperatures, due primarily to an increase in the curing residual stresses. Laminated plate theory, in conjunction with maximum stress criteria, appears to overestimate the onset of the transverse cracking in this laminate.					
15. SUBJECT TERMS polymer matrix composites, graphite/epoxy composites, mechanical testing, acoustic emission, cryogenic testing, coefficient of thermal expansion, transverse cracking, fracture toughness					
16. SECURITY CLASSIFICATION OF:			17. LIMITATION OF ABSTRACT: SAR	18. NUMBER OF PAGES 30	19a. NAME OF RESPONSIBLE PERSON (Monitor) L. SCOTT THEIBERT 19b. TELEPHONE NUMBER (Include Area Code) (937) 255-9070
a. REPORT Unclassified	b. ABSTRACT Unclassified	c. THIS PAGE Unclassified			

TABLE OF CONTENTS

Section		Page
	EXECUTIVE SUMMARY	1
1	INTRODUCTION	2
2	EXPERIMENTAL	4
	2.1 Thermomechanical Characterization	4
	2.2 Coefficient of Thermal Expansion (CTE)	5
	2.3 Fracture Toughness	5
	2.4 Onset of Microcracking	6
3	RESULTS	9
	3.1 Strength and Modulus	9
	3.2 Coefficient of Thermal Expansion	11
	3.3 Fracture Toughness	13
	3.4 Onset of Transverse Cracking	15
4	CONCLUSIONS	18
	REFERENCES	19
	LIST OF ACRONYMS	20

LIST OF FIGURES

Figure		Page
1	Acoustic Emission Record for $[0_2/90_2]_S$ Laminate at 23°C	7
2	Photograph Showing Failure of $[90]_{8T}$ Laminate	9
3	Photograph Showing Failure of $[\pm 45]_{2S}$ Laminate	10
4	Stress-Strain Curves for $[0]_{8T}$	10
5	Stress-Strain Curves for $[90]_{8T}$	10
6	Shear Stress-Strain Curves	11
7	Longitudinal Thermal Strain versus Temperature	12
8	Transverse Thermal Strain versus Temperature	12
9	Thermal Strain versus Temperature for $[0_2/90_2]_S$	13
10	Mode I Critical Energy Release Rate for IM7/977-3 at Room Temperature	15
11	Mode II Critical Energy Release Rate for IM7/977-3 at Room Temperature (left) and -196°C (right)	15
12	Transverse Cracks in $[0_2/90_2]_S$ Laminate	16

LIST OF TABLES

Table		Page
1	Variation of Strength and Modulus at Various Temperatures	9
2	CTE as a Function of Temperature	12
3	Calculated 90° Ply Stress and Strength	17

FOREWORD

This report was prepared by the University of Dayton Research Institute under Air Force Contract No. F33615-95-D-5029, Delivery Order No. 0007. The work was administered under the direction of the Nonmetallic Materials Division, Materials and Manufacturing Directorate, Air Force Research Laboratory, Air Force Materiel Command, with Dr. L. Scott Theibert (AFRL/MLBC) as Project Engineer.

This report was submitted in May 2001 and covers work conducted from 15 September 1999 through 1 March 2001.

EXECUTIVE SUMMARY

The application of composites in space structures, such as reusable launch vehicles (RLVs), requires a detailed understanding of their mechanical behavior and damage resistance in the service environment. Experimental and analytical studies were conducted on IM7/977-3, a toughened graphite/epoxy, to characterize the influence of cryogenic service temperatures on the strength, modulus, and fracture of this material system, and on transverse crack initiation in cross-ply laminates at 23, -129, and -196°C. Transverse tensile and shear strengths and moduli increased at the cryogenic test temperatures while strain to failure decreased, denoting increased brittleness. The stress for the onset of transverse cracking decreased substantially at cryogenic temperatures, due primarily to an increase in the curing residual stresses. Laminated plate theory, in conjunction with maximum stress criteria, appears to overestimate the onset of the transverse cracking in this laminate.

1. INTRODUCTION

Advanced polymer composites are being explored for structural applications at extremely low temperatures – for example, in large cryogenic fuel tanks on NASA’s RLV and on the U.S. Air Force’s Space Operations Vehicle [1]. Exposure to these cryogenic temperatures can cause transverse microcracking in these composites due to thermal residual stresses that arise from the anisotropy in the composite ply coefficient of thermal expansion (CTE). Transverse cracking often results in a reduction in laminate stiffness and strength and changes in laminate CTE, and provides a pathway for the ingress of moisture or corrosive chemicals; in cryotanks, transverse cracking can cause leakage of the pressurized liquid fuel. Very little work has been reported in the technical literature [2-4] on the mechanical performance of and damage development in polymer composites at cryogenic temperatures. The main objective of this work was to understand the mechanical behavior and damage processes in composites at cryogenic temperatures, and to develop a predictive capability for the onset of transverse cracking in composite laminates subjected to isolated or combined thermal and mechanical loads. The material system investigated was a carbon fiber-reinforced toughened epoxy composite, IM7/977-3. The thermomechanical properties required for the analysis were obtained from tests on $[0]_{8T}$, $[90]_{8T}$, and $[\pm 45]_{2S}$ laminates. These laminates were tested at a number of temperatures, ranging from ambient down to -196°C , using a custom-built cryogenic chamber installed on a mechanical test machine. Cross-ply laminates were used to experimentally determine the onset of transverse cracking under isolated or combined mechanical and thermal loads. Transverse cracking was detected from acoustic emission and incremental loading and unloading, and confirmed from microscopic examination of polished specimen edges. Ply stresses were calculated for the corresponding conditions from laminated plate theory, using the appropriate

experimentally generated thermomechanical properties and the applied load. The maximum stress failure theory was applied to predict failure. Analytical predictions were then compared with experimental results at temperatures of 23, -129, and -196°C, and the results are reported here.

2. EXPERIMENTAL

2.1 Thermomechanical Characterization

The material system used in this study was a carbon fiber-reinforced toughened epoxy, IM7/977-3, supplied as a unitape prepreg by the manufacturer. Unidirectional ($[0]_{8T}$ and $[90]_{8T}$) and multidirectional ($[\pm 45]_{2S}$ and $[0_2/90_2]_S$) laminates were fabricated in an autoclave in accordance with the manufacturer's recommended cure cycle. Cured composite panels were postcured for seven hours at 232°C in an oven. The $[0]_{8T}$, $[90]_{8T}$ and $[\pm 45]_{2S}$ laminates were used to characterize this composite material at cryogenic temperatures and provide the thermomechanical properties required for analytical calculation. The $[0_2/90_2]_S$ laminate was used to investigate transverse crack initiation in this composite system at cryogenic temperatures. Rectangular coupons were sectioned from the panels using a diamond-impregnated saw blade. All $[0]_{8T}$ specimens, as well as all specimens tested at -196°C, were 1.25 cm wide with a gage length of 10 cm due to size limitations imposed by the test fixture. All the remaining specimens had a width of 2.5 cm. Fiberglass/epoxy end-tabs were bonded to $[0]_{8T}$ and $[\pm 45]_{2S}$ specimens tested at 23 and -129°C; no end-tabs were used for specimens tested at -196°C. An axial strain gage was used to determine the elastic modulus and strain to failure at all test temperatures.

A special mechanical grip (17.8 kN load capacity) was designed and built for tests at cryogenic temperatures. The clamping face of each grip was coated using a Surfalloy process to enhance the gripping action without damaging the specimen surface by grip force. This grip can accommodate specimens with a width up to 1.25 cm. All specimens were tested on an MTS test machine using a commercial temperature chamber for tests at -129°C and a stainless-steel container, designed and built in-house, for tests at liquid nitrogen temperature (-196°C). Specimens, mounted on the test machine, were cooled to the desired test temperature by

immersion in liquid nitrogen in the insulated stainless-steel container and allowed to equilibrate for 20 minutes. They were then loaded in tension at a strain rate of 0.02/min.

2.2 Coefficient of Thermal Expansion

Composite CTEs were measured using strain gages, in conjunction with a computer-controlled temperature chamber and data acquisition system, continuously over the temperature range of 149 to -129°C, and then immersed in liquid nitrogen (-196°C) and liquid helium (-269°C) to record thermal strains at the corresponding temperatures. Ultralow-expansion titanium silicate was used as the reference material for completion of the strain gage bridge circuit. The details of this technique of CTE measurement using strain gages may be found elsewhere [5].

2.3 Fracture Toughness

Mode I double cantilever beam (DCB) tests and Mode II end notch flexure (ENF) tests were conducted to assess the interlaminar fracture properties under cryogenic temperatures. Tests were conducted at room temperature and liquid nitrogen temperatures (-196°C). The Mode I and Mode II test methodology and data reduction techniques are well documented in the literature and by other organizations (for example, [6, 7]).

Panels of unidirectional tape carbon/epoxy Cytec IM7/977-3 were fabricated and autoclave processed according to the established manufacturer's procedures. The panels were laid up with a stacking sequence of $[0]_{24T}$. Additionally, Kapton inserts were implanted along the midplane of the plates, near the edge of the panels, to later serve as crack initiators. Specimens were then fabricated for both DCB testing for Mode I interlaminar fracture toughness, as well as ENF testing for Mode II interlaminar fracture toughness. The room temperature tests were conducted in an ambient lab environment at a displacement rate of 0.02 mm/sec. At room

temperature the crack length was monitored using optical magnification of the specimen edges. For the cryogenic testing, the specimen was submerged in liquid nitrogen (using a specially fabricated stainless-steel tub) for a minimum of 10 minutes prior to starting each test. In these tests the crack length could not be monitored optically as before. Therefore, at each estimated 12.7-mm increment of crack growth, the test was stopped and the load removed. The cryogen was allowed to evaporate, and then the specimen was removed from the fixture and the actual crack length measured and noted. This process was then repeated four or five times for each specimen.

The ENF test was adopted for the measurement of Mode II critical energy release rate. Again, standard test procedures were used, including the introduction of a Mode I precrack by wedging the specimen open 2.54 mm past the Kapton insert. A loading rate of 0.04 mm/sec. was used, and a compliance calibration of the test specimen was performed by running tests of specimens of various crack lengths (actually accomplished by sliding the specimen a fixed amount and rerunning the test using the same specimen). Typically, specimens were loaded until failure occurred, resulting in a rapid load drop and the extension of the initial crack to near the center of the specimen. Typically, five specimens of each material and condition were tested. In several instances only four specimens were available for tests.

2.4 Onset of Microcracking

The edges of the $[0_2/90_2]_S$ specimens were first ground with sandpaper and then polished with 5-micron and 1-micron polishing powder to enhance microscopic imaging for crack detection. Prior to testing, all specimen edges were examined under a microscope to determine if specimen sectioning and handling induced any damage. No damage was observed in any specimen prior to testing. Acoustic emission was employed to detect the onset of microcracking

in tests conducted under ambient conditions. When a sudden acoustic emission event was observed, the specimen was unloaded and examined under a microscope to confirm the presence of transverse cracking. Figure 1 shows the acoustic emission record for a specimen tested at 23°C, indicating the occurrence of transverse cracking.

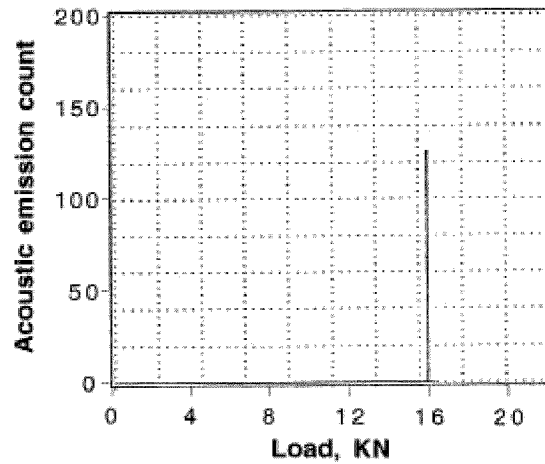


Figure 1. Acoustic Emission Record for $[0_2/90_2]_S$ Laminate at 23°C.

It should be noted that no other acoustic events were recorded in Figure 1, indicating no ambient noise during the test. The use of acoustic emission to detect microcracking was unsuccessful at -129°C, because of relatively high background noise, and at -196°C because of limitations of the transducer. Transverse crack initiation was therefore determined by microscopic examination of the polished specimen free edges after a series of incremental loading and unloading experiments. In this procedure a specimen is loaded to a stress level slightly lower than that at which microcracking is expected, then unloaded and the free edges examined in a microscope. If no microcracks are observed, the specimen is reloaded to a stress incrementally higher than before, unloaded, and examined again. This procedure is repeated until the first crack is observed, which is usually accomplished in two to five iterations. The average value of the last two consecutive loads is then used to compute the stress required to

initiate transverse cracking. With this procedure the error in the computed stress for crack initiation is less than five percent.

3. RESULTS

3.1 Strength and Modulus

The results of composite modulus and strength measurements are summarized in Table 1.

Table 1
Variation of Strength and Modulus at Various Temperatures

Laminate	Temperature °C	Strength MPa	Coefficient of Variation, %	Modulus GPa
Longitudinal [0] _{8T}	23	2,599	4.2	180
	-129	2,425	10.1	183
	-196	x	x	x
Transverse [90] _{8T}	23	66.1	6.7	9.8
	-129	76.3	22.1	13.0
	-196	94.6	5.6	13.2
Shear [±45] _{2S}	23	113.3	5.6	6.1
	-129	130.5	3.1	8.1
	-196	132.1	5.4	9.2

There is a considerable variation in modulus and strength, especially in matrix-dominated directions, over the temperature range of 23 to -196°C. The longitudinal modulus, from [0]_{8T} specimens, did not change in the temperature range, but longitudinal strength decreased by seven percent at -129°C. Both moduli and strengths for the [90]_{8T} and [±45]_{2S} orientations increase significantly at the lower test temperatures, as seen in Table 1. Analysis of the fracture modes indicated increasingly brittle failure at the lower temperatures. Figures 2 and 3 show photographs of failed [90]_{8T} and [±45]_{2S} specimens tested at 23 and -196°C.

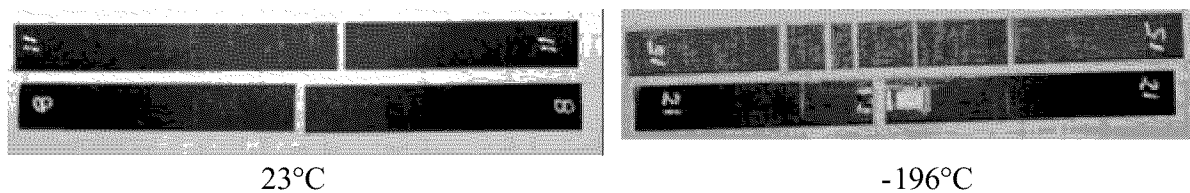


Figure 2. Photograph Showing Failure of [90]_{8T} Laminate.

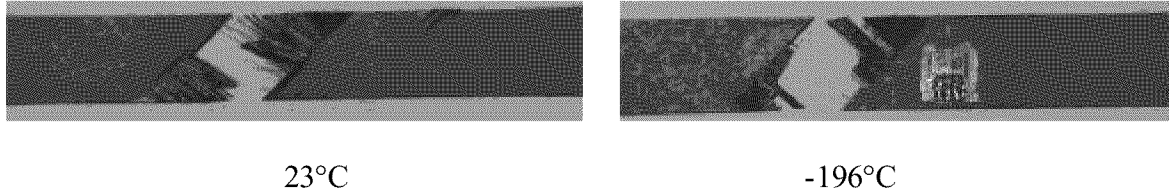


Figure 3. Photograph Showing Failure of $[\pm 45]_{2S}$ Laminate.

Multiple failures were observed in some $[90]_{8T}$ specimens at -129 and -196°C, whereas each specimen tested at 23°C exhibited a single failure. The failure modes of the $[\pm 45]_{2S}$ specimens also clearly showed the increased brittleness at -196°C.

The longitudinal stress-strain curves at 23 and -129°C, shown in Figure 4, are linear and practically coincide. The transverse stress-strain curves for the test temperatures 23, -129, and -196°C, shown in Figure 5, indicate an increase in modulus at lower temperatures. The stress-strain behavior of the $[\pm 45]_{2S}$ laminate shows a wide range of nonlinearity over the range of test temperatures; the nonlinearity gradually decreases with test temperature until the plot is almost linear (up to failure) at the lowest temperature as shown in Figure 6.

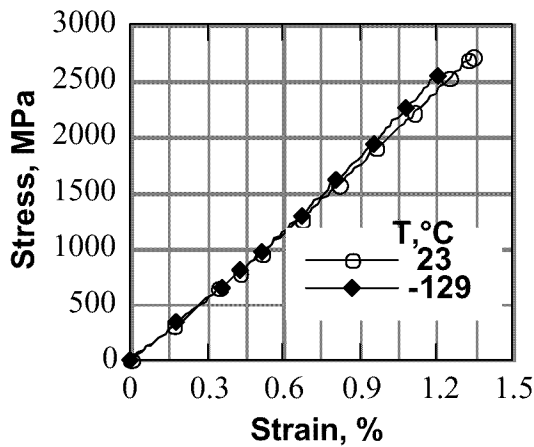


Figure 4. Stress-Strain Curves for $[0]_{8T}$.

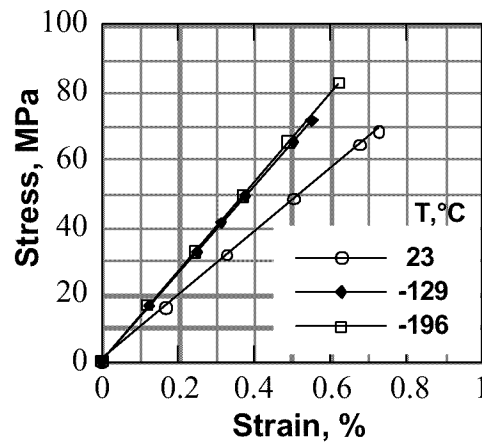


Figure 5. Stress-Strain Curves for $[90]_{8T}$.

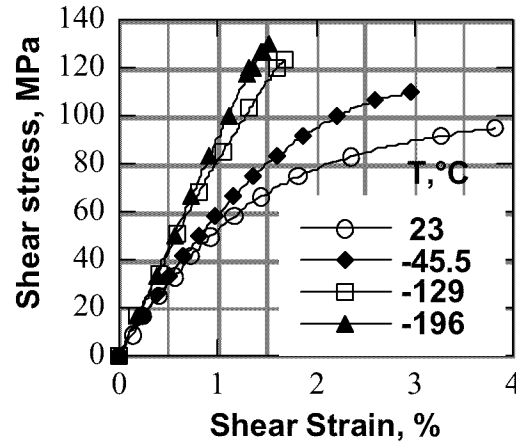


Figure 6. Shear Stress-Strain Curves.

3.2 Coefficient of Thermal Expansion

The coefficient of thermal expansion (CTE) for the material system was determined from the measured thermal strains using the strain gage technique. Figures 7 and 8 show the longitudinal and transverse thermal strains as function of temperatures, respectively.

Both longitudinal and transverse thermal strains show some degree of nonlinear behavior in the extreme temperatures. Since we are interested in calculating the residual stresses in the interested ply within a laminate, the CTEs were determined on the basis of the strain difference between cure and interested temperatures. Table 2 shows the longitudinal CTE, α_L , and transverse CTE, α_T , determined.

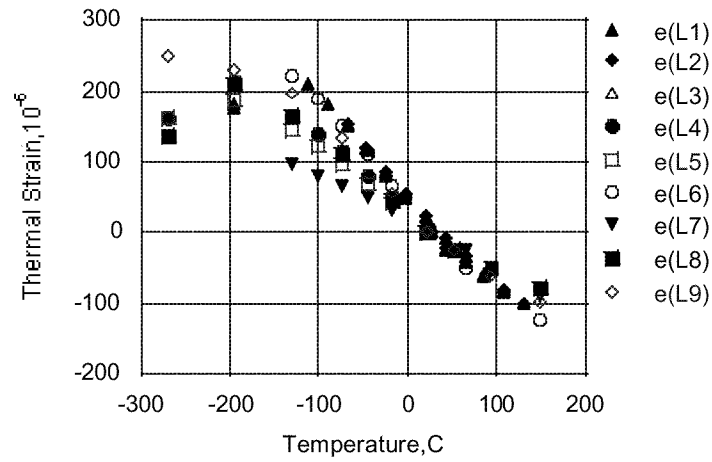


Figure 7. Longitudinal Thermal Strain versus Temperature. (L1, ..., L9 represent the individual specimens.)

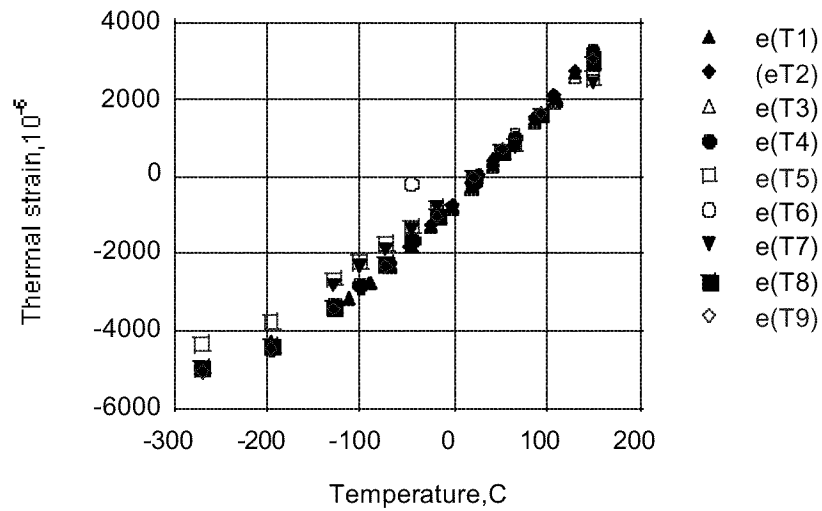


Figure 8. Transverse Thermal Strain versus Temperature. (T1, ..., T9 represent the individual specimens.)

Table 2
CTE as a Function of Temperature

	Temperature, °C		
	23	-129	-196
$\alpha_L, 10^{-6}/^{\circ}\text{C}$	0.18	0.17	0.15
$\alpha_T, 10^{-6}/^{\circ}\text{C}$	23.4	22.1	19.8

Figure 9 shows the thermal strain versus temperatures for the $[0_2/90_2]_s$ laminate. The CTEs determined for this sample are also indicated in this figure. L and T in Figure 9 represent longitudinal and transverse directions with respect to the fiber direction of the surface layer, respectively. Both specimens, designated 1 and 2, show a greater CTE in the transverse direction than in the longitudinal direction. The calculated CTE value of this laminate using the laminated plate theory and unidirectional CTEs is $2.0 \times 10^{-6}/^\circ\text{C}$, which is intermediate between the measured longitudinal and transverse values for both specimens.

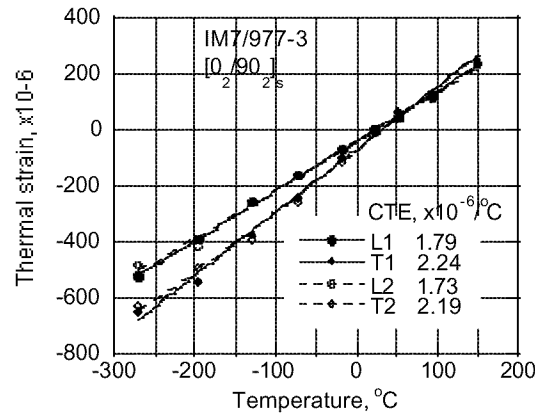


Figure 9. Thermal Strain versus Temperature for $[0_2/90_2]_s$.

3.3 Fracture Toughness

Test data for the DCB specimens were reduced using two techniques: the compliance calibration method and the area method [6-7]. The compliance calibration technique essentially uses the changing specimen compliance in the $\partial C/\partial a$ term of the fracture equation:

$$G_{Ic} = (P^2/2b) \partial C/\partial a, \quad (1)$$

where G_{Ic} is the Mode I critical energy release rate, P is the load at failure, b is the specimen width, a is the crack length, and C is the specimen compliance given by the following:

$$C = \delta/P, \quad (2)$$

where δ is the specimen displacement at the point of load application. It can be noted that the compliance method used in the DCB test data reduction utilizes the curve-fitted actual compliance change in each specimen tested. The area method simply utilizes the area in the load-displacement curve as the energy used in creating a crack increment of known measured length.

Data reduction in the ENF tests similarly uses Equations (1) and (2), with the exception that the compliance change term $\partial C/\partial a$ is developed subsequent to the actual fracture tests. In addition, a compliance curve was developed for both material types under each of the two temperature conditions, resulting in four compliance calibration curves.

The test results are depicted in Figures 10 and 11. Figure 10 depicts the Mode I DCB results for IM7/977-3 at both room temperature and -196°C. Note that the Mode I energy release rate, G_{Ic} , is plotted as a function of crack length. This was done to determine if a dependency of G_{Ic} on crack length existed, such as might be the case if significant fiber bridging were to occur. As can be seen in the figure, the G_{Ic} values for both the room temperature and -196°C cases are fairly constant with respect to crack length. The room temperature tests indicate a G_{Ic} of approximately 219 J/m², while the -196°C tests show a drop in G_{Ic} to 131 J/m².

The Mode II results for G_{IIc} in IM7/977-3 are shown in Figure 11. Note that the room temperature results show very little scatter and a level of G_{IIc} of approximately 753 J/m². In contrast, the results at -196°C indicate a drop in Mode II toughness, with an overall level of about 630 J/m² and more scatter than the room temperature data.

An examination of the fracture surfaces indicated a possible reason for the loss in G_{Ic} for the 977-3 at the cold condition. Other changes in toughness values, both G_{Ic} and G_{IIc} , were inconclusive.

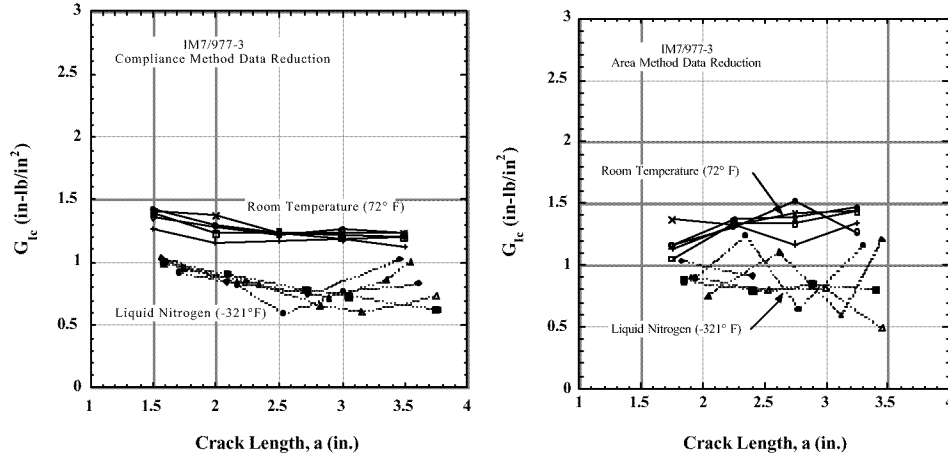


Figure 10. Mode I Critical Energy Release Rate for IM7/977-3 at Room Temperature. Data reduced using the compliance method (left) and area method (right).

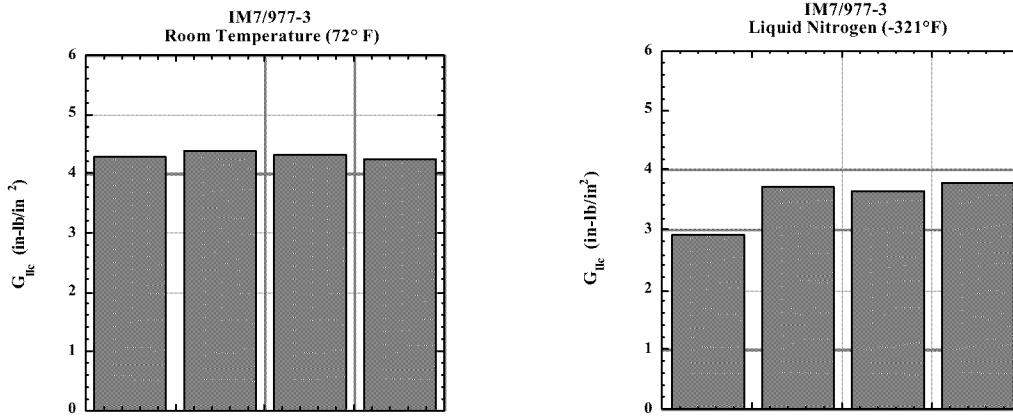
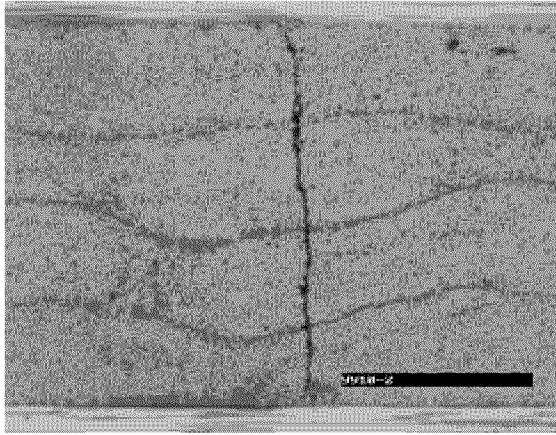


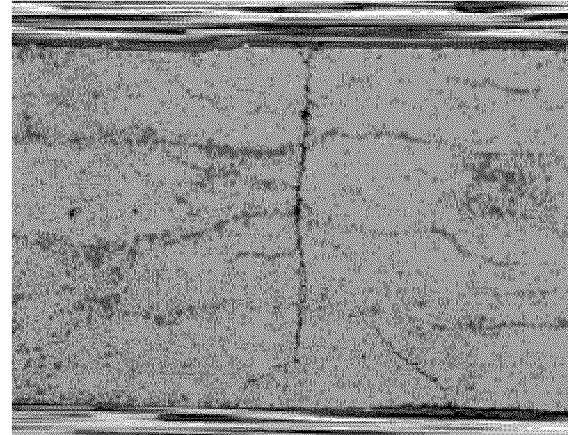
Figure 11. Mode II Critical Energy Release Rate for IM7/977-3 at Room Temperature (left) and -196°C (right).

3.4 Onset of Transverse Cracking

All of the transverse cracks observed on the specimen edge extended through the entire thickness of the 90° plies, as shown in Figure 12. There was a one-to-one mapping of cracks on both edges of the same specimen, suggesting that these transverse cracks traversed the full specimen width.



23°C



-196°C

Figure 12. Transverse Cracks in $[0_2/90_2]_S$ Laminate.

In specimens tested at -196°C , a slanted partial crack was also observed near the major transverse crack (Figure 12); this damage was not observed in specimens tested at 23 and -129°C . The stress in the 90° plies of the $[0_2/90_2]_S$ laminate, at the onset of transverse cracking, was calculated from the applied stress using classical laminated plate theory for comparison with the transverse strength obtained from tensile tests on $[90]_{8T}$ specimens. The curing residual stress, taking into account the influence of water absorbed under ambient storage conditions, was calculated with the assumption of a stress-free temperature of 163°C (cure temperature 177°C). The moisture content of the composite, absorbed during storage between fabrication and testing, was determined to be 0.15 percent. Table 3 shows the 90° ply stresses calculated for the $[0_2/90_2]_S$ laminate at the onset of transverse cracking, and the measured composite transverse strength.

The total stress represents the stress calculated from the laminate stress (applied load) at the onset of transverse cracking and the curing residual stress. It can be seen that the predictions, based on a maximum stress failure criterion from lamination theory, are considerably overestimated especially for tests conducted at -129°C . A number of factors such as the

Table 3
Calculated 90° Ply Stress and Strength

Temperature °C	Curing Residual Stress MPa	Mechanical Stress @ Cracking Load MPa	Total Stress MPa	90° Ply Strength MPa
23	17.8	60.4	78.2	74.5
-129	45.6	52.3	97.9	83.4
-196	60.3	51.8	112.1	97.3

constraining effect of neighboring plies, ply thickness, inadequacy of the failure criteria, inaccuracies in the estimation of residual stress, insufficient data on transverse strengths and stress for the onset of transverse crack initiation may contribute to the discrepancy between prediction and experiment. A fracture mechanics approach, which accounts for some of the above factors, is currently being explored using analytical models [8-9] in conjunction with additional experimental data.

4. CONCLUSIONS

Experimental and analytical studies were conducted to determine the influence of cryogenic temperatures on the strength and modulus of IM7/977-3, a graphite-toughened epoxy composite, and the initiation of transverse cracking in cross-ply laminates. Based on the results, the following conclusions are drawn:

1. Transverse tensile and shear strengths and moduli increased at lower temperatures while strain to failure decreased (indicating increased brittleness).
2. The nonlinearity of the shear stress-strain curve decreased significantly at lower temperatures.
3. The stress level at the onset of transverse cracking decreased significantly at lower temperatures, mainly due to an increase in the curing residual stresses. Residual stress relief due to absorbed moisture was taken into account.
4. The Mode I fracture toughness significantly decreased at -196°C , and the Mode II results indicated a measurable drop at -196°C .
5. Lamination theory in conjunction with the maximum stress failure criterion tends to overestimate the onset of the transverse cracking in this laminate.
6. The strain gage technique is an easy and accurate means of measuring composite CTE at cryogenic temperatures.
7. Specimen alignment, especially for transverse loading, is critical due to specimen embrittlement at cryogenic temperatures.

REFERENCES

1. Heydenreich, R. (1998). Cryotanks in Future Vehicles. *Cryogenics* 38 (125-130).
2. Reed, R. P., & M. Golda. (1994). Cryogenic Properties of Unidirectional Composites. *Cryogenics* 34 (909-928).
3. Schultz, J. B. (1998). Properties of Composite Materials for Cryogenic Applications. *Cryogenics* 38 (3-12).
4. Ishikawa, T., H. Kumazawa, Y. Morino, & Y. Hayashi. (1998). Cryogenic Strength Behavior of Toughened Composites for Propellant Tank of Reusable Launch Vehicle. *ACCM* 1.
5. Kim, R. Y., A. S. Crasto, & G. A. Schoeppner. (1997). Measured and Predicted Variation in Laminate CTE due to Microcracking. *Proc. of American Society for Composites* 12 (1103-1112).
6. Standard Test Method for Mode I Interlaminar Fracture Toughness of Unidirectional Fiber-Reinforced Polymer Matrix Composites. *ASTM D5528-94A*.
7. Test Procedure for the End Notched Flexure (ENF) Test. *ASTM D30.02 Round Robin*.
8. Lim, S. C., & C. S. Hong. (1989). Prediction of Transverse Cracking and Stiffness Reduction in Cross-Ply Laminated Composites. *J. Compos. Mater.* 23 (695-713).
9. Pagano, N. J., G. A. Schoeppner, R. Y. Kim, & F. L. Abrams. (1998). Steady-State Cracking and Edge Effects in Thermomechanical Transverse Cracking of Cross-Ply Laminates. *Composite Science and Technology* 58 (1811-1823).

LIST OF ACRONYMS

CTE	Coefficient of thermal expansion
DCB	Double cantilever beam
ENF	End notch flexure
MTS	Materials Testing Systems
PMC	Polymer matrix composite
RLV	Reusable launch vehicle